SAND--91-0381C

DE91 009763

S-PARAMETER MEASUREMENTS AND APPLICATIONS OF SUPERCONDUCTING FLUX FLOW TRANSISTORS

J. S. Martens, V. M. Hietala, T. E. Zipperian, D. S. Ginley, and C. P. Tigges - Sandia National Laboratories, Department 1140, Albuquerque, NM 87185

J. M. Phillips

AT&T Bell Labs, 600 Mountain Avenue, Murray Hill, NJ 07974

ABSTRACT

We have performed microwave two-port S-parameter measurements and modelling on Superconducting Flux Flow Transistors (SFFTs). These transistors, based on the magnetic control of flux flow in an array of High Temperature Superconducting (HTS) weak links, can exhibit significant available power gain at microwave frequencies (over 20 dB at 7-10 GHz in some devices). The input impedance is largely inductive while the output impedance is both resistive and inductive. The characteristics are such that these devices are potentially useful in numerous applications including matched amplifiers.

INTRODUCTION

The SFFT is an active four terminal superconducting device that has been studied for several years (e.g.,[1]-[7]). The device exhibits very high speed operation (10-30 ps transit times with 3 μm minimum feature size), large gain and impedance levels that are useful for many applications. The present work concentrates on small signal S-parameter measurements of these devices and a discussion of a SFFT application, matched amplifiers, that can be better analyzed with these new data.

DEVICE BASICS

The SFFT consists of a parallel array of weak superconducting links (separating two unweakened superconducting electrodes) and a control line to provide a local magnetic field. An example of this structure is shown in Fig. 1. The links are typically 2-3 μm wide by 10 μm long and 50-90 nm thick (while the electrodes are at least 200 nm thick). The number of links does not strongly affect performance but larger numbers of links help by lowering output resistance and slightly increasing device gain at the expense of frequency response [7]. When the device is biased below the critical current, typically 0.5-5.0 mA, no flux is admitted into the link system (perfect Meissner state). Above the critical current, flux is admitted in discrete quanta known as vortices[8]. These vortices can flow since the bias current generates a Lorentz-type force on the vortices. The vortices are also subject to forces from external magnetic fields (from the control line), viscous damping, pinning forces (which are undesirable in that the average vortex speed is reduced) and surface barriers at the edges of the links which hamper flux entry and exit. The balance of these forces determines the flux motion and hence the terminal voltage. In terms of active device performance, the key principle is the use of an external magnetic field (via the control line) to modulate the flux density in the link system [9],[10], the resulting flux motion, and hence the terminal voltage.

The device are made from films of TlCaBaCuO and YBaCuO on $LaAlO_3$ substrates. The TlCaBaCuO films were made by sequential e-beam evaporation followed by sintering in air under a partial pressure of Tl-O and annealing in oxygen. The process is described in detail elsewhere [11]. The Tl samples used in these experiments had T_c's of about 103K and critical current densities at 77K (0 field) of about 350 kA/cm^2 (1 μV/cm DC criterion). In making the YBaCuO films, Y and Cu metals are evaporated from separate electron gun sources and BaF_2 is resistively evaporated [12]. During co-deposition of these three materials, the chamber is backfilled with dry O_2. The films are annealed ex-situ in a carefully optimized multi-stage process [13]. The YBCO films used in these experiments had T_c's of about 90K and critical current densities at 77K (0 field) of about 1 MA/cm^2.

I-V curves for two of the devices (one made of TlCaBaCuO and one of YBaCuO) tested are shown in Fig. 2. The current through the link system (or body) is denoted by I_{bdy} while the control current is labeled I_c. The two most important circuit parameters to be drawn from these curves are the transresistance ($\Delta V/\Delta I_c = r_m$) and output resistance ($\Delta V/\Delta I_{bdy} = r_o$). For the microwave measurements, the devices will be biased at about 8 mA on the 'body' and 0.2 mA on the control line where typical values are $r_m \approx 17$-$19\ \Omega$ and $r_o \approx 3$-$4\ \Omega$. An equivalent circuit based on device physics is shown in Fig. 3 [7]. Since moving flux generates a voltage and the impetus is a control current, a transresistance is the active element for the equivalent circuit. The moving vortices have normal cores and hence represent an ohmic resistance (r_o). The input and output impedances are both inductive because of the geometry of the structures and, for the output inductance, because of the excess kinetic inductance of the thin superconducting film in the link region[14]. The values of these and other parasitics are discussed after the measurements section.

S-PARAMETER MEASUREMENTS

The first measurements were made with Cascade signal-ground probes using SOTL (short, open, thru, load) calibration [15]. This probing scheme presented problems because of planarity requirements and the irregularity of the $LaAlO_3$ substrates used. As a result, contacting was difficult. Data was obtained for one Tl device at 77K with some effort and these results are summarized in Fig. 4. The roughness of the maximum transducer gain (MTG) [16] is due largely to unstable contacts (particularly in the liquid nitrogen environment). There are, however, some interesting features of this data. S_{21} is reasonably large in magnitude and $|S_{21}|>>|S_{12}|$ indicating active behavior. The measurement of these two parameters was relatively repeatable (to within ≈1 dB) and at least semi-quantitatively correct since an unbiased device showed $|S_{12}|=|S_{21}| \approx$ -40 dB across the band. The MTG, while having some uncertainty, does indicate the possibility of large gain with adequate matching.

Custom probes using Cascade mounts and spring-loaded pogo launchers in a ground-signal-ground configuration were designed to circumvent contacting problems. These probes, though still not perfected, did allow for highly repeatable measurements below 10 GHz. Dual-band TRL (thru, short, delay) calibration [15] at 77K was employed. The 77K S-parameters for the two devices (whose IV curves are in Fig. 2) are shown in Fig. 5. The bias point (I_{bdy}=8 mA, I_c=0.2 mA) was chosen because r_m was nearing its plateau value and r_o was still relatively small. As would be expected from the equivalent circuits, the input and output impedances are low and inductive. S_{21} behaves as with the device of Fig. 4 but $|S_{12}|$ is larger. This is largely due to poor isolation with our present probe design. To verify the isolation problem, both probes were placed on a shorting block about the same distance apart from each other as during the transistor measurement and the S-parameters were measured. The measured $|S_{12}|$ and $|S_{21}|$ are shown in Fig. 6 and indicate the poor isolation which is undoubtedly masking the true transistor S_{12}. The actual device S_{12} is probably like that shown in Fig. 4. This error in S_{12} will skew the MTG calculations. One sample (using the actual measured device data) is shown in Fig. 7 which, even with the S_{12} error, the MTG exceeds 14 dB. We expect 20-25 dB is closer to the actual MTG over this band.

Model parameters can be determined by fitting the equivalent circuit to the data of Fig. 5. After removing launch parasitics (obtained by looking at a device electrode configuration with no SFFT in place), the equivalent circuit of Fig. 3 was fit to the data for the YBCO device (Fig. 5b). The control line was found to be adequately modeled by a 0.3 nH input inductance and an input resistance of 0.2 Ω. The other model parameters include $r_m \approx 18.2\ \Omega$, $r_o = 3.7\ \Omega$, and $L_{out} \approx 0.17$ nH. This fitting process was repeated for the Tl device at different bias levels and the results are shown in Table 1. As is apparent, the output resistance, transresistance, and output inductance are all reasonably strong functions of bias. The transresistance reaches a relatively broad plateau while the output resistance and inductance are somewhat more volatile. The dependence of the output inductance on control current is suitable for phase shifting.

AN APPLICATION

Because of the relatively large transresistance and low impedances, a matched amplifier could show very high gains[6]. The most recent results are shown in Fig. 8 using the device of Fig. 5b. A maximum gain of about 13 dB was achieved with a return loss of 9 dB at midband. The matching attempt was not to achieve MTG but to get as much gain as possible with about 1 GHz of bandwidth and a center frequency of about 4 GHz. The matching in this case was done with normal transmission line sections for convenience but superconducting matching networks have been used previously [6] and have insertion loss advantages. Since the impedance mismatch is rather severe, relatively high currents will be flowing on the device side of the matching net and any normal conductor losses will become significant.

CONCLUSIONS

We have presented S-parameter measurements of a superconducting flux flow transistor. They indicate that are large amount of power gain is available but significant matching must be employed. An example was given showing an amplifier with over 13 dB gain a bandwidth of roughly 1 GHz at a center frequency of 4 GHz. Multistage and distributed structures are currently being investigated. Other applications including synthetic transmission line phase shifters (using the SFFT's variable output inductance), active impedance convertors [4] and mixers [7] have been successfully tried as well.

ACKNOWLEDGEMENTS

This work was supported by the U.S. Department of Energy through Sandia National Laboratories under contract No. DE-AC04-76P00789 and by DARPA, ONR and SDI under contract No. N0017390WR00172. The authors would like to thank Gert Hohenwarter of the University of Wisconsin-Madison and Parkview Works of Milton, WI for motivating some of the probing techniques and for useful discussions.

REFERENCES

1 G. K. G. Hohenwarter, J. S. Martens, D. P. McGinnis, J. B. Beyer, J. E. Nordman, and D. S. Ginley, " Single superconducting thin film devices for applications in high T_c materials circuits," IEEE Trans. on Mag., vol. MAG-25, pp. 954-956, Mar 1989.

2. J. S. Martens, G. K. G. Hohenwarter, J. B. Beyer, J. E. Nordman, and D. S. Ginley, "S parameter measurements on single superconducting thin-film three-terminal devices made of high-T_c and low T_c materials," J. Appl. Phys., vol. 65, pp. 4057-4060, May 1989.

3. J. S. Martens, J. B. Beyer, J. E. Nordman, G. K. G. Hohenwarter, and D. S. Ginley, "A superconducting single film device oscillator made of high T_c and low T_c materials," Proceedings of the 1989 International IEEE MTT-S Symposium, pp. 443-446, Jun 1989.

4. J. S. Martens, J. B. Beyer, J. E. Nordman, G. K. G. Hohenwarter and D. S. Ginley, "A Josephson Junction to FET High Speed Line Driver made of Tl-Ca-Ba-Cu-O," to be published in IEEE Trans. on Mag, vol. MAG-27, Mar 1991.

5. J. S. Martens, J. B. Beyer, J. E. Nordman, and D. S. Ginley, "A broadband microwave linear phase modulator made of high T_c superconductors," Micr. and Opt. Tech. Lett., vol. 3, pp. 49-51, Feb 1990.

6. G. K. G. Hohenwarter, J. S. Martens, J. B. Beyer and J. E. Nordman, "Resonant Impedance Matching of Abrikosov Vortex-Flow Transistors," to be published in IEEE Trans. on Mag, vol. MAG-27, Mar 1991.

7. J. S. Martens, "The Model and Applications of a High Frequency Three Terminal Device Made of High Temperature Superconductors," PhD Dissertation, University of Wisconsin-Madison, May 1990.

8. K. K. Likharev, "Vortex motion and the Josephson effect in superconducting thin bridges," Sov. Phys. - JETP, vol. 34, pp. 906-912, Apr 1972.

9. T. Van Duzer and C. W. Turner, Principles of Superconductive Devices and Circuits, New York: Elsevier, 1981, Chp. 8.

10. J. Pearl, "Current distribution in superconducting films carrying quantized fluxoids," Appl. Phys. Lett., vol. 5 , pp. 65-66, Jul 1964.

11. D. S. Ginley, J. F. Kwak, E. L. Venturini, B. Morosin and R. J. Baughman, "Morphology control and high critical currents in superconducting thin films in the Tl-Ca-Ba-Cu-O system," Physica C, Vol. 160, pp. 42-48, Oct 1989.

12. M. P. Siegal, J. M. Phillips, Y. F. Hsieh and J. H. Marshall, "Growth of epitaxial $Ba_2YCu_3O_{7-x}$ films on $LaAlO_3$ (001)," Physica C, vol. 172, pp. 282-286, Dec 1990.

13. M. P. Siegal, J. M. Phillips, R. B. van Dover, T. H. Tiefel and J. H. Marshall, "Optimization of annealing parameters for the growth of epitaxial $Ba_2YCu_3O_{7-x}$ films on $LaAlO_3$ (001),"J. Appl. Phys., vol. 68, pp. 6353-6360, Dec 1990.

14. T. Van Duzer and C. W. Turner, Principles of Superconductive Devices and Circuits, New York: Elsevier, 1981, Chp. 3.

15. " On-wafer measurements using the HP 8510 network analyzer and Cascade Microtech wafer probes," Hewlett Packard, Product Note 8510-6, 1986.

16. G. Gonzalez, Microwave Transistor Amplifiers, Englewood Cliffs, NJ: Prentice-Hall, chp. 3, 1984.

17. J. S. Martens, D. S. Ginley, T. E. Zipperian, V. M. Hietala, and C. P. Tigges, "Novel applications of Tl-Ca-Ba-Cu-O thin films to active and passive high frequency devices," presented at the 1990 International Symposium on Superconductivity, 12 November 1990, Sendai, Japan.

FIGURE CAPTIONS

Figure 1. Layout of the superconducting flux flow transistor. Port 1 is the control line and port 2 is the device body.

Figure 2. IV curves of two SFFTs (a) a TlCaBaCuO device, (b) a YBaCuO device. I_{bdy} is the current through the device body (link region) and I_c is the control current. The voltage V is measured across the link system.

Figure 3. An equivalent circuit of the SFFT. Values of the components are discussed in the text. The transresistance component is the active element. Other interesting features include the non-linearity of the output inductor and the low amount of cross-talk (M is typically 10 pH or so).

Figure 4. Measured S-parameters (a) and computed Maximum transducer gain (b) for a Tl SFFT probed with Cascade signal-ground probes. Note the low cross-talk and large available gain. The roughness of MTG is due to contacting problems. For all MTG plots, maximum available gain is used when the device is stable and maximum stable gain is used otherwise.

Figure 5. Measured S-parameters of a TlCaBaCuO device (a) and a YBaCuO device (b) probed using the spring-loaded structure described in the text. In both cases, the bias conditions were I_{bdy}=8.0 mA and I_c= 0.2 mA. The data shows inductive input and output impedances (low in magnitude) and a higher $|S_{21}|$ due largely to the probes. On the Smith charts, the outer curve is S_{11} while the inner curve is S_{22}.

Figure 6. Measured $|S_{21}|$ and $|S_{12}|$ of the two probes (spring-loaded) placed on a shorting block separated by the spacing used in the Fig. 5 experiments. This shows the true $|S_{12}|$ of the devices is probably no higher than that of Fig. 4 results.

Figure 7. Computed Maximum Transducer Gain of the devices measured for Fig. 5. (a) TlCaBaCuO device and (b) YBaCuO device. Even with the error in S_{12}, the MAG exceeds 13 dB.

Figure 8. Performance of a matched amplifier constructed with the device of Fig. 5B. Maximum gain of 13 dB was achieved with a bandwidth of almost 1 GHz.

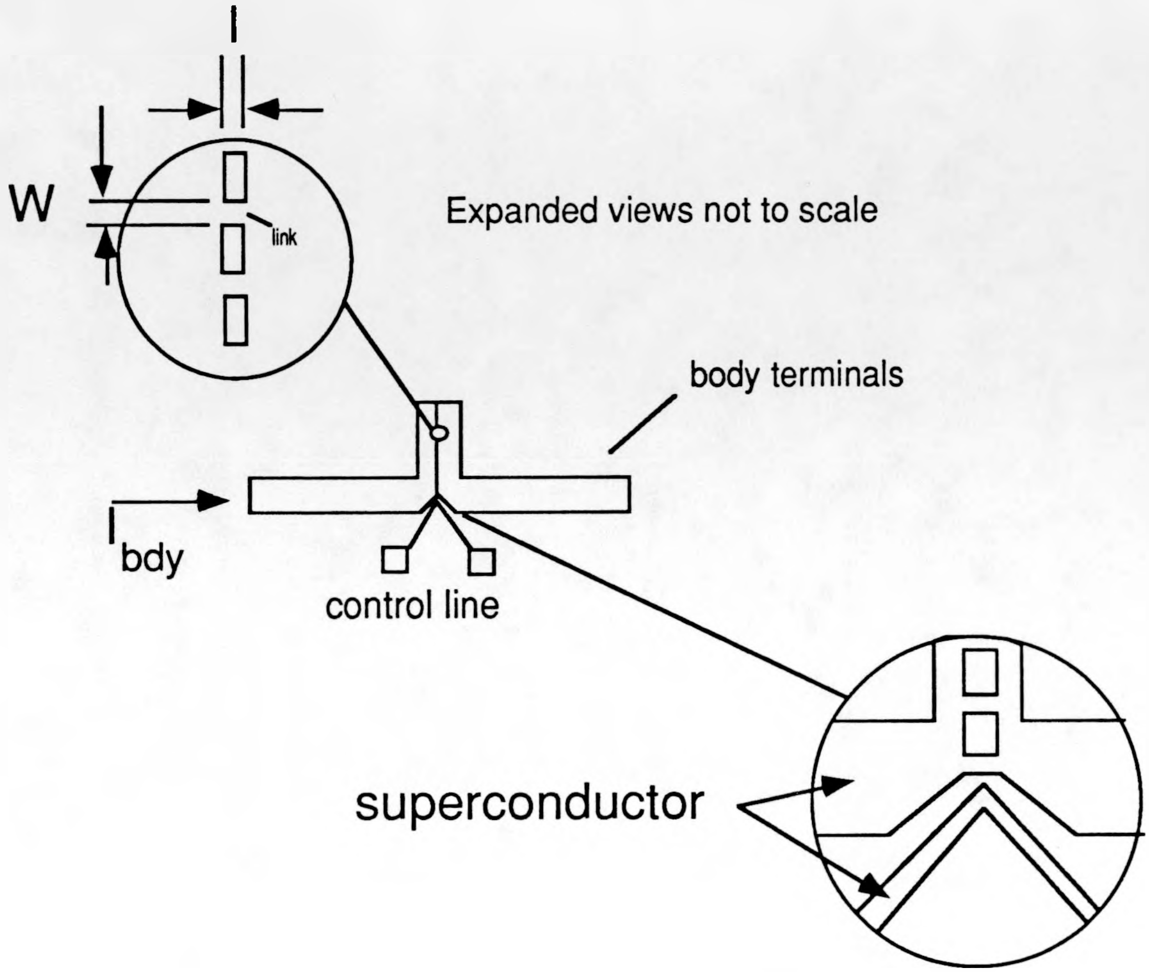
l
W
link
Expanded views not to scale
body terminals
I
bdy
control line
superconductor

Figure 1

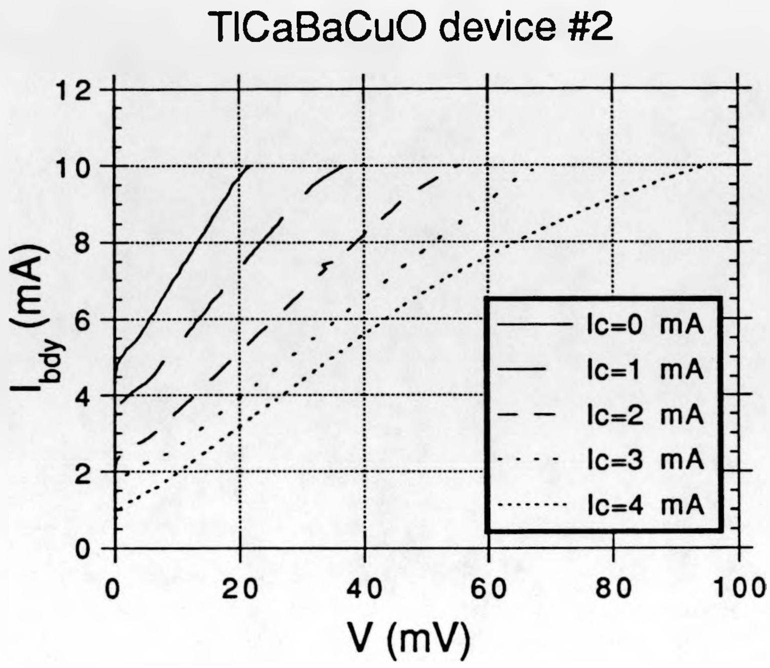
TlCaBaCuO device #2
I_{bdy} (mA)
V (mV)
0
2
4
6
8
10
12
0
20
40
60
80
100
Ic=0 mA
Ic=1 mA
Ic=2 mA
Ic=3 mA
Ic=4 mA

Figure 2A

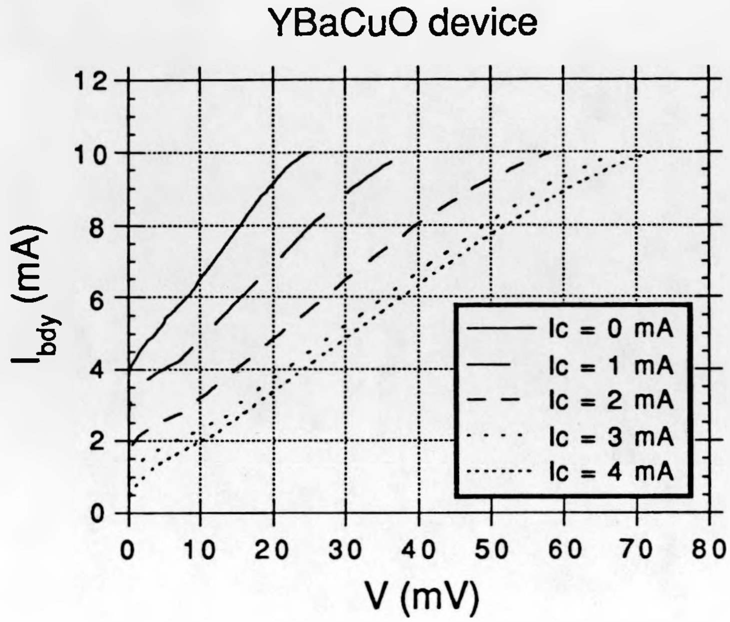
YBaCuO device
I_{bdy} (mA)
V (mV)
0
2
4
6
8
10
12
0
10
20
30
40
50
60
70
80
Ic = 0 mA
Ic = 1 mA
Ic = 2 mA
Ic = 3 mA
Ic = 4 mA

Figure 2B

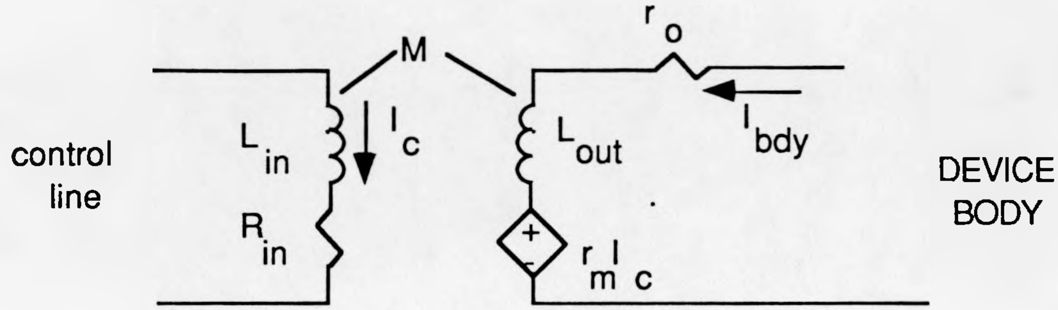

Figure 3

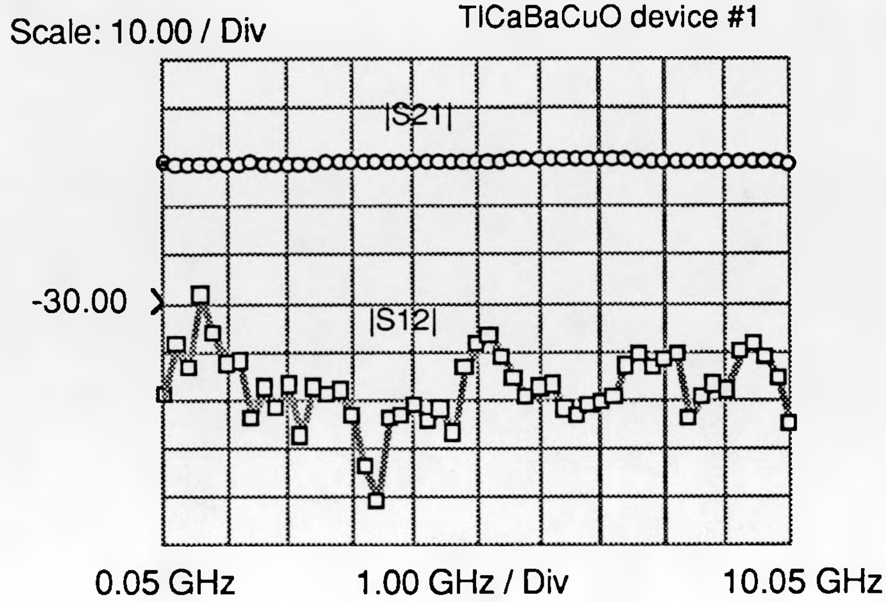

Figure 4A

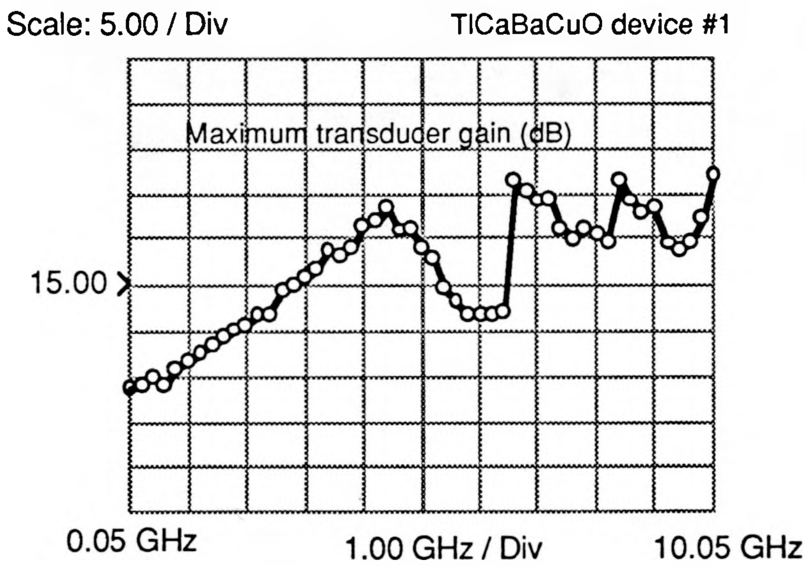

Figure 4B

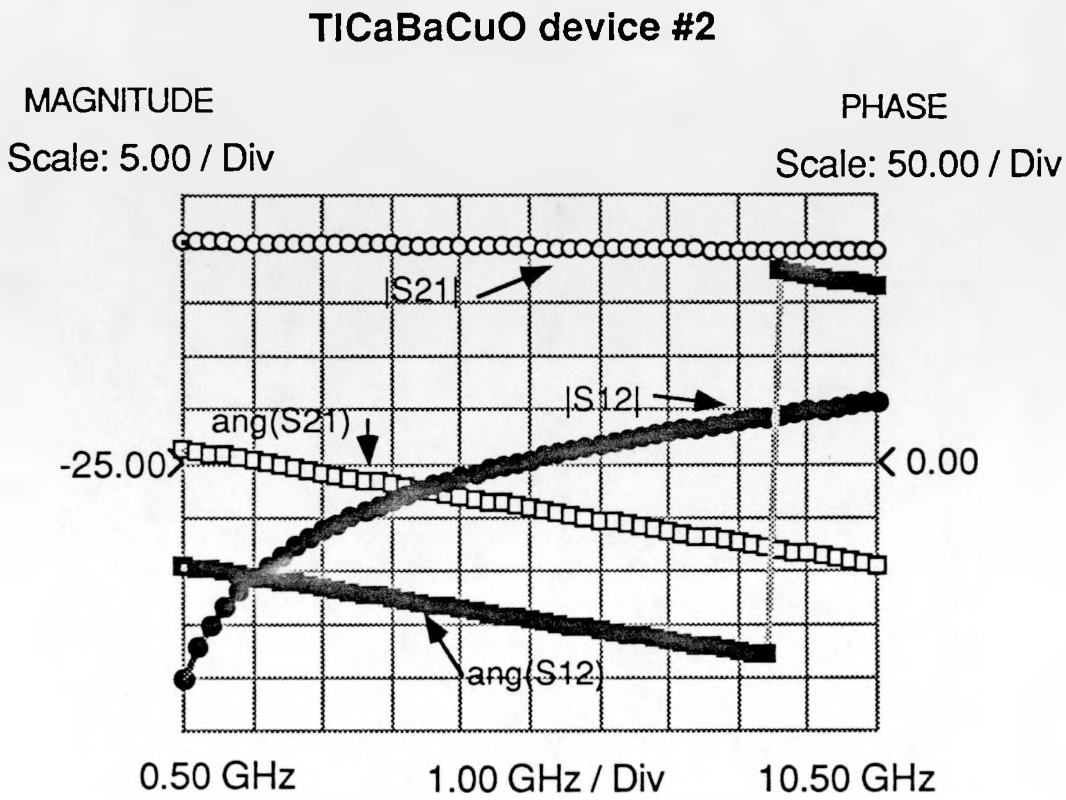
TlCaBaCuO device #2
MAGNITUDE
Scale: 5.00 / Div
PHASE
Scale: 50.00 / Div
|S21|
|S12|
ang(S21)
-25.00
0.00
ang(S12)
0.50 GHz
1.00 GHz / Div
10.50 GHz

Figure 5A

Microwave Lab™
© 1989 Lightwave Technologies, Inc.

hts32ab.ckt
Output #2

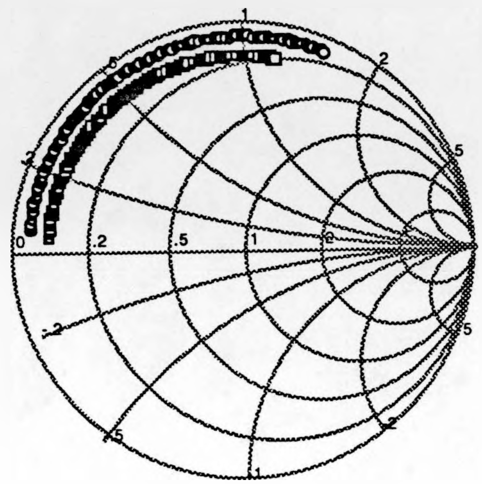

Figure 5A (cont.)

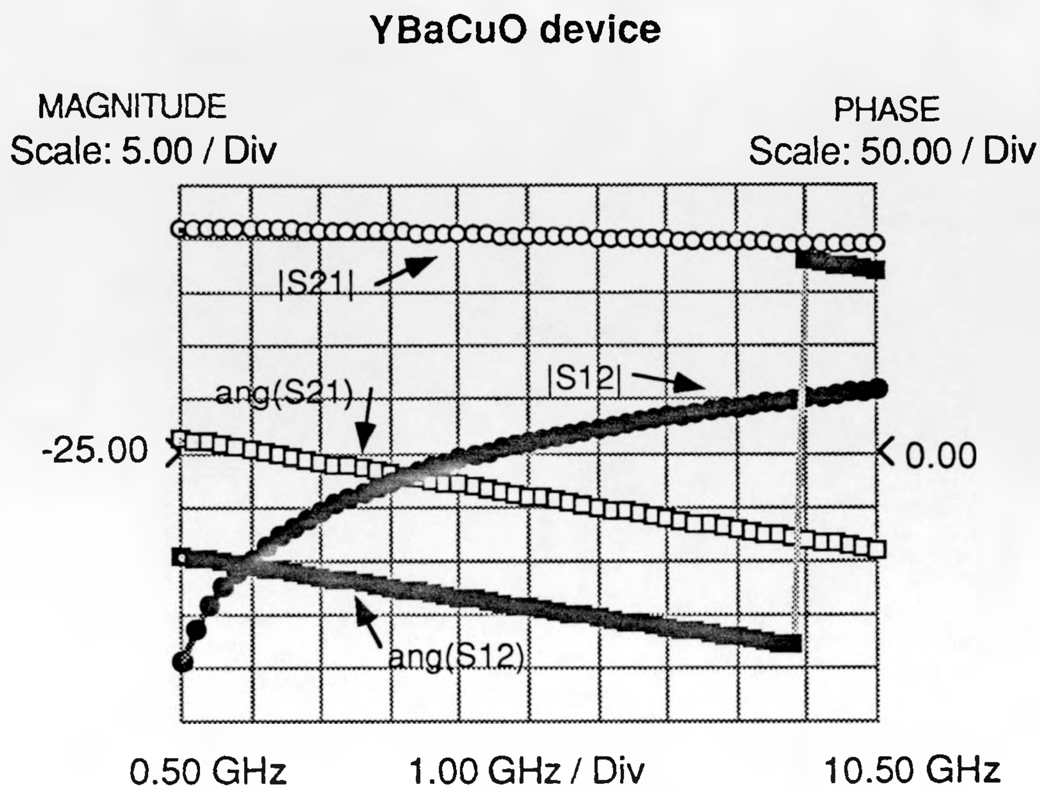
YBaCuO device
MAGNITUDE
Scale: 5.00 / Div
PHASE
Scale: 50.00 / Div
|S21|
|S12|
ang(S21)
-25.00
0.00
ang(S12)
0.50 GHz
1.00 GHz / Div
10.50 GHz

Figure 5B

Microwave Lab™
© 1989 Lightwave Technologies, Inc.

hts41ab.ckt
Output #2

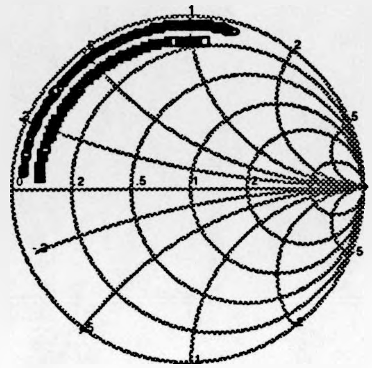

Figure 5B (cont.)

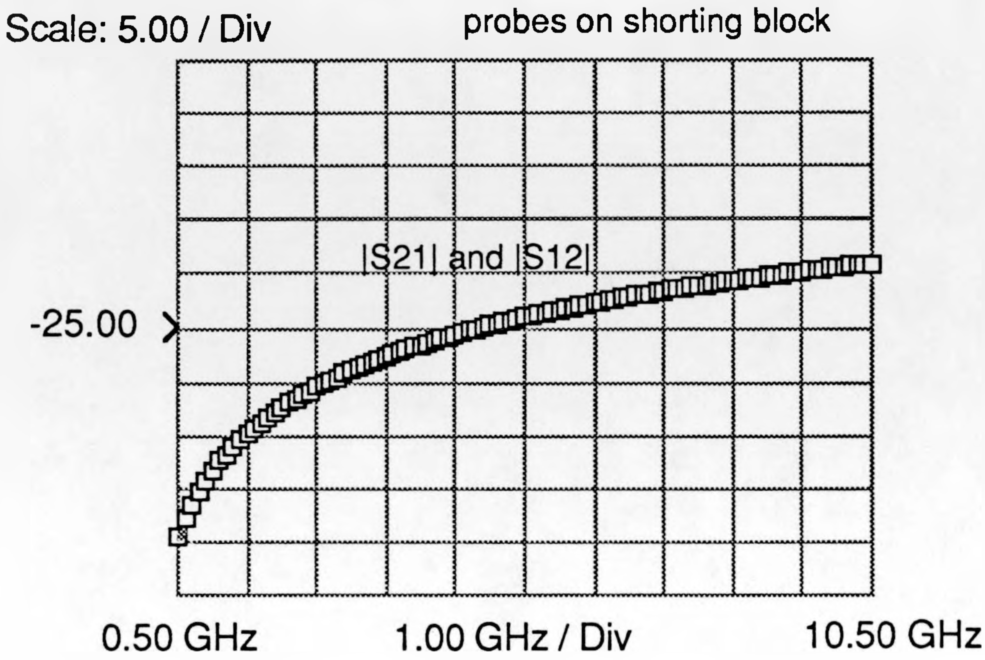

Scale: 5.00 / Div
probes on shorting block
|S21| and |S12|
-25.00
0.50 GHz
1.00 GHz / Div
10.50 GHz

Figure 6

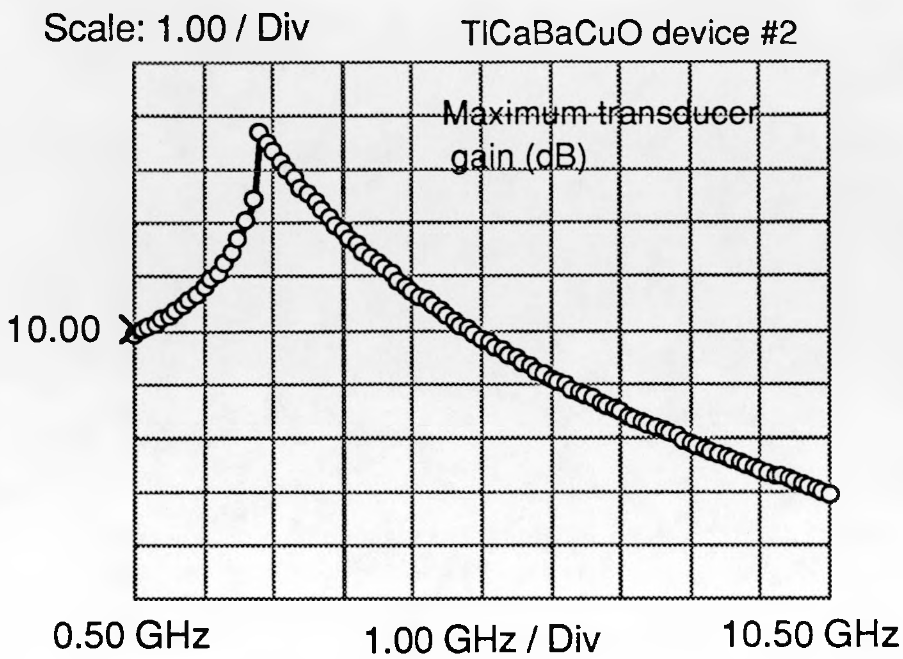
Scale: 1.00 / Div
TlCaBaCuO device #2
Maximum transducer gain (dB)
10.00
0.50 GHz
1.00 GHz / Div
10.50 GHz

Figure 7A

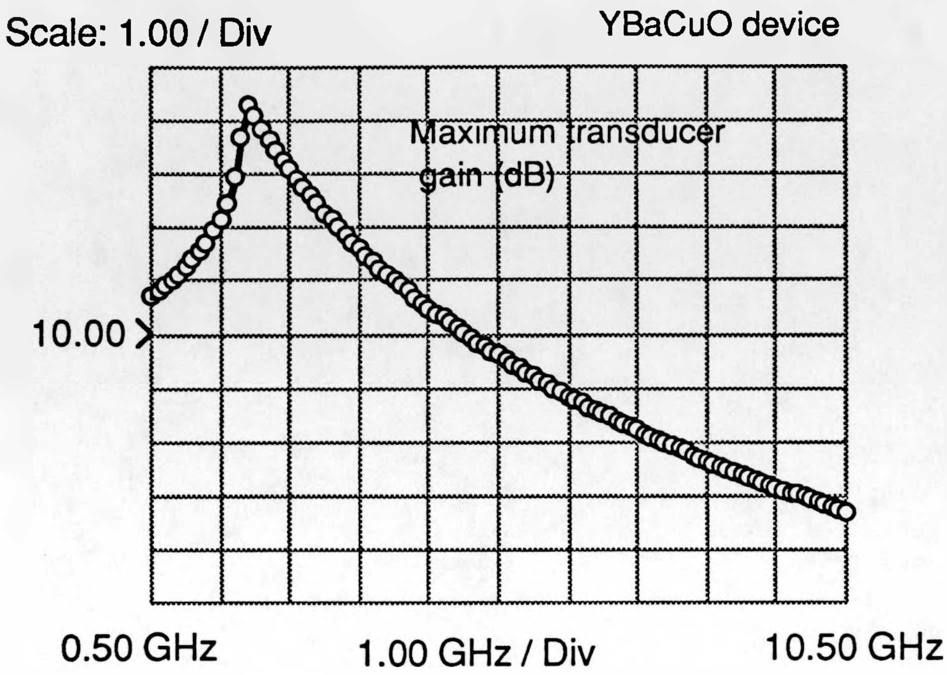
Scale: 1.00 / Div
YBaCuO device
Maximum transducer
gain (dB)
10.00
0.50 GHz
1.00 GHz / Div
10.50 GHz

Figure 7B

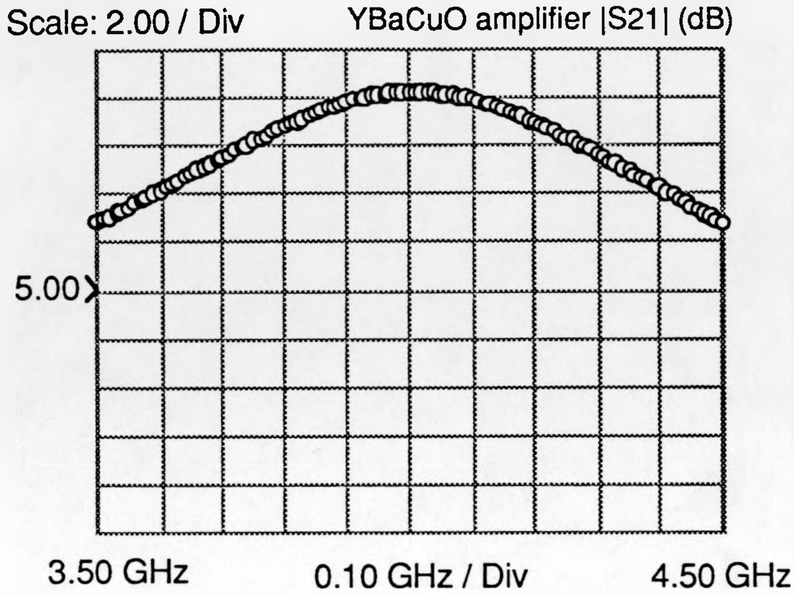
Scale: 2.00 / Div
YBaCuO amplifier |S21| (dB)
5.00
3.50 GHz
0.10 GHz / Div
4.50 GHz

Figure 8

Tl sample equivalent circuit parameters

I_{bdy} (mA)	I_c (mA)	r_m (Ω)	r_o (Ω)	L_{out}(nH)	L_{in}(nH)	R_{in}(Ω)
6.0	0.2	10.2	3.9	0.65	0.3	0.1
8.0	0.2	17.8	4.0	0.49	0.3	0.1
10.0	0.2	18.0	4.5	0.32	0.3	0.1
6.0	2.5	6.8	9.3	0.30	0.3	0.1
8.0	2.5	8.8	9.7	0.18	0.3	0.1
10.0	2.5	9.2	10.1	0.1	0.3	0.1

TABLE 1.. Equivalent circuit parameter values for the device of Fig. 5a at various bias levels. Note the variability of the output inductance and resistance and the plateau that r_m quickly reaches.